

# Numerical Study of Excited States in the Shastry-Sutherland Model

Tomo MUNEHISA and Yasuko MUNEHISA

*Faculty of Engineering, Yamanashi Univ., Kofu 400-8511*

(Received November 6, 2018)

We investigate excited states of the Shastry-Sutherland model using a kind of variational method. Starting from various trial states which include one or two triplet dimers, we numerically pursue the best evaluation of the energy for each set of quantum numbers. We present the energy difference as a function of either the coupling ratio or the momentum and compare them with the perturbative calculations. Our data suggest that the helical order phase exists between the singlet dimer phase and the magnetically ordered phase. In comparison with the experimental data we can estimate the intra-dimer coupling  $J$  and the inter-dimer coupling  $J'$  for  $\text{SrCu}_2(\text{BO}_3)_2$ :  $J'/J = 0.65$  and  $J = 87\text{K}$ .

KEYWORDS: Shastry-Sutherland model, excited states, variational method, dispersion, helical order

## 1. Introduction

One of recent fascinating topics in two-dimensional quantum spin systems is the Shastry-Sutherland model (SS model),<sup>1)</sup> the model of orthogonal dimers with the intra-dimer coupling  $J$  ( $> 0$ ) and the inter-dimer coupling  $J'$  ( $> 0$ ). This model provides a nontrivial system which relates an exactly solvable spin-gaped model obtained in the  $J' \rightarrow 0$  limit to a square lattice model where intra-dimer interaction vanishes ( $J = 0$ ). It is known that the exact ground state of the SS model is the direct product of the singlet dimers when  $J' \leq J'_c \sim 0.68J$ , while for the sufficiently large  $J'/J$  the system is in the magnetic order phase with the Néel ground state.

A lot of notable studies have been done on this system since Kageyama *et al.*<sup>2)</sup> found that  $\text{SrCu}_2(\text{BO}_3)_2$  realizes the SS model and its coupling ratio  $J'/J$  is very close to the critical value of the model. Active experimental works have reported additional interesting features of this matter such as magnetization plateaus,<sup>2-4)</sup> magnetic-field dependence of the thermal conductivity,<sup>5,6)</sup> and soundwave anomalies.<sup>7)</sup>

Theoretical investigation was stimulated by Miyahara and Ueda<sup>8)</sup> who pointed out the locality of the excited states in the SS model. Owing to the expectation that this locality should account for the observed magnetization plateaus, many calculations based on the perturbative methods<sup>9-14)</sup> have been carried out. Although their results qualitatively agree with the experimental data,<sup>15-18)</sup> the expansion parameter, estimated to be  $0.6 - 0.7$  for  $\text{SrCu}_2(\text{BO}_3)_2$ , seems too large to ensure the validity of the perturbation. Therefore non-perturbative approaches are desired in order to confirm discussions on the excited states.

In this paper we show numerical results obtained by a variational method, which we have recently developed and named the operator variational (OV) method,<sup>19,20)</sup> together with the restructuring technique.<sup>21,22)</sup> Our purpose is to study the lowest excited state of the SS model on a square lattice sketched in Fig. 1. Using the OV method we can perform systematic calculations without damaging the quantum symmetries of the system. The trial states, on the other hand, should be given by inspection. We examine some of the one-triplet states and the two-triplet states with the total spin  $S = 0, 1$  and  $2$ , paying special attentions to the symmetries of the system's Hamiltonian on lattices equally sized in the  $x$  and the  $y$  directions. We see that the value of the lowest energy, which provides an upper bound of the true value, strongly depends on the choice of the trial state. We therefore employ various trial states and adopt the one whose energy is the lowest among them.

Our results indicate several interesting features on the dispersion relations and on the phase transition of the model. They are in good accordance with the perturbative results if the inter-dimer coupling is weak, but discrepancies are observed when we move on toward the transition point. It is likely that the helical order phase<sup>23,24)</sup> exists. Trying a comparison with experimental data on  $\text{SrCu}_2(\text{BO}_3)_2$  we obtain several encouraging results.

In section 2 we introduce the SS model and discuss its symmetry used to distinguish the states. Section 3 is to give a brief description on the OV method and to comment on its application to the SS model. Numerical results on  $8^2$  and  $12^2$  lattices are presented in section 4 and the final section is devoted to summary and discussions. In appendices A-E we show the trial states employed in our numerical study.

## 2. Model and Symmetry

In the Shastry-Sutherland model a spin is located at every site of the lattice schematically shown in Fig. 1, whose coordinates are denoted by either

$$(2n_x a \pm \frac{d}{2}, 2n_y a \pm \frac{d}{2}) \quad (A \text{ sublattice}) \quad \text{or} \quad ((2n_x + 1)a \pm \frac{d}{2}, (2n_y + 1)a \mp \frac{d}{2}) \quad (B \text{ sublattice})$$

with  $n_x, n_y = 0, 1, \dots, N_{eff} - 1$ , where  $N_{eff}$  is the number of dimers,  $2a$  is the unit distance between dimers and  $d$  is the distance between two spins of a dimer. The total number of spins  $N$  therefore equals to  $4N_{eff}^2$ .

The Hamiltonian of this model is given by

$$\begin{aligned} \hat{H} &= \frac{1}{4}J \sum_{n_x, n_y=0}^{N_{eff}-1} \{h_a(n_x, n_y) + h_b(n_x, n_y)\} \\ &+ \frac{1}{4}J' \sum_{n_x, n_y=0}^{N_{eff}-1} \{h_1(n_x, n_y) + h_2(n_x, n_y) + h_3(n_x, n_y) + h_4(n_x, n_y)\}, \end{aligned} \quad (1)$$

where,  $\sigma(x, y)$  being the Pauli matrix at the location  $(x, y)$ ,

$$h_a(n_x, n_y) \equiv \sigma(2n_x a + \frac{d}{2}, 2n_y a + \frac{d}{2}) \cdot \sigma(2n_x a - \frac{d}{2}, 2n_y a - \frac{d}{2}), \quad (2)$$

$$h_b(n_x, n_y) \equiv \sigma((2n_x + 1)a + \frac{d}{2}, (2n_y + 1)a - \frac{d}{2}) \cdot \sigma((2n_x + 1)a - \frac{d}{2}, (2n_y + 1)a + \frac{d}{2}), \quad (3)$$

$$h_1(n_x, n_y) \equiv \sigma(2n_x a + \frac{d}{2}, 2n_y a + \frac{d}{2}) \cdot \{\sigma((2n_x + 1)a + \frac{d}{2}, (2n_y + 1)a - \frac{d}{2}) + \sigma((2n_x + 1)a - \frac{d}{2}, (2n_y + 1)a + \frac{d}{2})\}, \quad (4)$$

$$h_2(n_x, n_y) \equiv \sigma(2n_x a - \frac{d}{2}, 2n_y a - \frac{d}{2}) \cdot \{\sigma((2n_x - 1)a + \frac{d}{2}, (2n_y - 1)a - \frac{d}{2}) + \sigma((2n_x - 1)a - \frac{d}{2}, (2n_y - 1)a + \frac{d}{2})\}, \quad (5)$$

$$h_3(n_x, n_y) \equiv \sigma((2n_x + 1)a + \frac{d}{2}, (2n_y + 1)a - \frac{d}{2}) \cdot \{\sigma((2n_x + 2)a + \frac{d}{2}, 2n_y a + \frac{d}{2}) + \sigma((2n_x + 2)a - \frac{d}{2}, 2n_y a - \frac{d}{2})\}, \quad (6)$$

$$h_4(n_x, n_y) \equiv \sigma((2n_x + 1)a - \frac{d}{2}, (2n_y + 1)a + \frac{d}{2}) \cdot \{\sigma(2n_x a + \frac{d}{2}, (2n_y + 2)a + \frac{d}{2}) + \sigma(2n_x a - \frac{d}{2}, (2n_y + 2)a - \frac{d}{2})\}. \quad (7)$$

Periodic boundary conditions are assumed in both  $x$  and  $y$  directions.

Symmetric operates to commute with the Hamiltonian are  $T_x$  (translation in the  $x$  direction),  $T_y$  (translation in the  $y$  direction),  $U$  ( $A$ - $B$  translation),  $V_x$  ( $A$ - $B$  translation in the  $x$  direction),  $V_y$  ( $A$ - $B$  translation in the  $y$  direction) and  $I_{\pm}$  ( $x$ - $y$  reflections), which translate  $\sigma(x, y)$  as follows.

$$T_x \sigma(x, y) T_x^\dagger = \sigma(x - 2a, y), \quad T_y \sigma(x, y) T_y^\dagger = \sigma(x, y - 2a),$$

$$U \sigma(x, y) U^\dagger = \sigma(-y - a, x + a),$$

$$V_x \sigma(x, y) V_x^\dagger = \sigma(-x - a, y + a), \quad V_y \sigma(x, y) V_y^\dagger = \sigma(x + a, -y - a),$$

$$I_+ \sigma(x, y) I_+^\dagger = \sigma(y, x), \quad I_- \sigma(x, y) I_-^\dagger = \sigma(-y, -x).$$

Note that

$$U^4 = \hat{1}, \quad I_+^2 = \hat{1}, \quad I_-^2 = \hat{1},$$

where  $\hat{1}$  denotes the unit operator, and

$$U = I_+ V_y = I_- V_x.$$

### 3. OV method

In this section we make a brief description of the OV method we proposed in ref.19, where we showed that this method enables us to calculate the energy for large quantum systems with less computer memory resources compared with the Lanczos method.

In the OV method, assuming that the Hamiltonian  $\hat{H}$  is the sum of  $N_g$  partial Hamiltonians  $\hat{g}_i$ ,

$$\hat{H} = \sum_{i=1}^{N_g} \hat{g}_i,$$

we systematically generate candidate operators

$$\hat{O}(k_1 \equiv 0, k_2, \dots, k_L) \equiv \sum_{i=1}^{N_g} \hat{g}_{i+k_1} \hat{g}_{i+k_2} \cdots \hat{g}_{i+k_L} \quad (L = 1, 2, \dots, L_{max}),$$

with some integer  $L_{max}$  and all possible values of integers  $k_2, k_3, \dots, k_L$ . Then we select a set of operators  $\{\hat{O}_i\} = \{\hat{O}_0 \equiv I(\text{Identity}), \hat{O}_1, \dots, \hat{O}_{n-1}\}$  from those candidates so that  $\hat{O}_0 | \Psi \rangle, \hat{O}_1 | \Psi \rangle, \dots, \hat{O}_{n-1} | \Psi \rangle$  includes all linearly independent states for the given  $L_{max}$  and  $| \Psi \rangle$ . Thus we obtain an approximate basis to calculate the Hamiltonian matrix elements. Once the basis is determined, the orthogonalization and the diagonalization are easily carried out by conventional methods.

Let us then concentrate our attention to trial states, the highly model-dependent component of the method. We study the dispersion in two cases. One is the case  $p_y = p_x$ , where we employ those states which have *even/odd* parity in the  $x$ - $y$  reflection  $I_+$ . They are one-triplet states with the total spin  $S = 1$ , two-nearest-neighboring-triplet states with  $S = 0, 1, 2$  (abbreviated as *nn*-triplet states hereafter) and two-next-nearest-neighboring-triplet states (*nnn*-triplet states hereafter) with  $S = 0, 1, 2$ . In the other case  $p_y = 0$ , the trial states are eigenstates of  $V_y$ , the operator to represent  $A$ - $B$  translation in the  $y$  direction. Details of these trial states are given in appendices.

#### 4. Results

Now we present our results obtained on  $8 \times 8$  and  $12 \times 12$  lattices ( $p_x$  or  $p_y$  being therefore 0,  $\frac{1}{3}\pi$ ,  $\frac{1}{2}\pi$ ,  $\frac{2}{3}\pi$  and  $\pi$ ) with  $L_{max} = 3$ . We did not find any size effect on the results with the same  $(p_x, p_y)$ , where  $p_x(p_y) = 0$  or  $\pi$ , calculated for these two lattice sizes.<sup>25,26)</sup>

In Fig. 2 we plot, as a function of the coupling ratio  $J'/J$ , the difference between the energy of the singlet-dimer state  $E_0$  and the lowest energy  $E$  for the momentum  $\mathbf{p}=(0,0)$ , the total spin  $S = j$  ( $j = 0, 1$ ) and the *even* or *odd*  $I_+$  parity. We determine  $E$  with  $S = 1$  as the minimum value among the energy calculated from the one-triplet trial states, the *nn*-triplet trial states and the *nnn*-triplet trial states which are explicitly described in the Appendices D and E. Let us introduce notations  $E_{min}^{one}$ ,  $E_{min}^{nn}$  and  $E_{min}^{nnn}$  to represent the minimum energy obtained from the one-, the *nn*- and the *nnn*-triplet trial states, respectively. Then the above is stated by  $E \equiv \min\{E_{min}^{one}, E_{min}^{nn}, E_{min}^{nnn}\}$ . As for the  $S = 0$  states we compare the *nn*- and the *nnn*-triplet trial states, namely  $E \equiv \min\{E_{min}^{nn}, E_{min}^{nnn}\}$ .

When  $\mathbf{p}=(0,0)$  it turned out for  $S = 1$  that  $E = E_{min}^{nn}$  and  $E$  is doubly degenerate, being independent on the  $I_+$  parity. Our results on the energy difference  $E - E_0$ , which correspond to the

spin gap for this value of  $S$ , nicely agree with the perturbative expansion up to the fifth order of  $J'/J$  (the dotted line in the figure) presented by Fukumoto.<sup>13)</sup> Especially for small values of  $J'/J$ , say for  $J'/J \leq 0.5$ , the agreement is excellent. When  $S = 0$ ,  $E$  is obtained from the  $nn$ -triplet trial states for the *odd*  $I_+$  parity in the whole range of the examined coupling ratio, while for the *even*  $I_+$  parity  $E = E_{min}^{nnn}$  if  $J'/J \geq 0.55$ . Both  $I_+$  parity results are also compatible with the ones based on the perturbation theory,<sup>12), 14)</sup>

A remarkable feature in Fig. 2 is a crossover between  $E$  with  $S = 0$ , *odd*  $I_+$  parity and  $E$  with  $S = 1$ . We see that the former, which is much larger than the latter when  $J'/J$  is 0.45, decreases more rapidly to reach  $E_0$  faster than the latter when the coupling ratio grows. This observation suggests the existence<sup>27)</sup> of the helical order phase<sup>23, 24)</sup> between  $r_1 < J'/J < r_2$ , where  $r_1$  ( $r_2$ ) is the value of the coupling ratio where  $E$  with  $S = 0$ , *odd*  $I_+$  parity (with  $S = 1$ , *even* and *odd*  $I_+$  parity) becomes equal to  $E_0$ . There are two reasons to believe that this crossover is not an artifact due to the approximations in the OV method but a real property of the SS model. One is that the exact calculations on small lattices (16 and 24 sites) also indicate this crossover. Another reason is that the  $S = 1$  results would be less affected by the higher order corrections than the  $S = 0$  ones because they are known to be more reliable in the coupling region around the crossover. Since the OV method is a kind of variational method, this means that we would observe more decrease of  $E$  in the  $S = 0$  case when  $L_{max}$  is increased. The crossover is thus expected to survive in more precise estimations. Quantitatively, the crossover point and the values of  $r_1$  and  $r_2$ , which are  $\simeq 0.65$ ,  $\simeq 0.75$  and  $\simeq 0.8$  in the present study, might change for the smaller in further numerical work.

Next we study how  $E$  depends on the momentum  $(p, p)$  or  $(p, 0)$ . In Figs. 3-5 we show dispersions of the energy difference calculated for  $\mathbf{p}=(p, p)$ ,  $S = j$  ( $j = 0, 1, 2$ ) and  $\mathbf{p}=(p, 0)$ ,  $S = 1$  with the coupling ratios  $J'/J = 0.5$  (Fig. 3), 0.6 (Fig. 4) and 0.65 (Fig. 5). Here we examine the one- and the  $nn$ -triplet trial states for  $S = 1$  and  $\mathbf{p}=(p, 0)$ , while for  $\mathbf{p}=(p, p)$  we calculate  $E \equiv \min\{E_{min}^{nn}, E_{min}^{nnn}\}$  ( $E \equiv \min\{E_{min}^{one}, E_{min}^{nn}, E_{min}^{nnn}\}$ ) when  $S = 0, 2$  ( $S = 1$ ).

Let us first direct our attention to the dispersions from the  $S = 1$  trial states. When  $\mathbf{p}=(p, p)$  we observe, at each coupling ratio stated above, that the lowest energy with even  $I_+$  parity is  $E_{min}^{nn}$  for all values of  $p$ . With odd  $I_+$  parity, on the other hand, we observe that  $E = E_{min}^{one}$  for  $0 < p < \pi$ . As was stated above, the lowest energy for  $p = 0$  is irrelevant to the  $I_+$  parity so that the system has doubly degenerate  $E(= E_{min}^{nn})$ . This degeneracy is also found at  $p = \pi$ . In another case  $\mathbf{p}=(p, 0)$ , we find that  $E_{min}^{nn}$  is slightly smaller than  $E_{min}^{one}$  when  $p = \pi$  while  $E_{min}^{nn} > E_{min}^{one}$  for all other values of  $p$ . The  $S = 1$  results in the figures indicate that the *even*  $I_+$  state is almost dispersionless. Its value changes only  $\sim 3\%$  even when the value of  $J'/J$  is as large as 0.65. We also see that the energy with the *odd*  $I_+$  state depends very weakly on  $p$ . Similar tendency is observed for the  $\mathbf{p}=(p, 0)$  state, too. This feature is in marked contrast to the reported perturbative work, where the dispersion is flat only for small values of the coupling ratio. For example, the dispersion

by Weihong *et al.*<sup>10)</sup> shows rapidly growing fluctuations near  $J'/J \sim 0.65$ .

Turning to results for  $S = 0$  state we see strong momentum dependence of  $E$  both for *even* and *odd*  $I_+$  parity, which is the very impressive characteristic of this state. Here  $E = E_{min}^{nn}$  always holds if the  $I_+$  parity is *odd*. For the *even*  $I_+$  parity, however, it depends on the values of  $J'/J$  and  $p$  whether  $E_{min}^{nn} < E_{min}^{nnn}$  or not. When the coupling ratio is 0.5 it turned out that  $E = E_{min}^{nn}$  whatever  $p$  is. On the other hand, we observe  $E_{min}^{nnn}$  underlies  $E_{min}^{nn}$  for  $J'/J = 0.6$ ,  $p = 0$  and for  $J'/J = 0.65$ ,  $p = 0$  or  $p = \pi/3$ . These dispersions are in qualitative agreement with those given by Totsuka *et al.*<sup>12)</sup> for  $J'/J=0.5$  and by Fukumoto<sup>13)</sup> for  $J'/J=0.55$ , although their values are smaller than ours.

Finally we comment on the  $S = 2$  case, where the relation  $E_{min}^{nnn} < E_{min}^{nn}$  is always observed.<sup>28)</sup> Both the *even* and the *odd*  $I_+$  parity dispersions are weakly dependent on the momentum in accordance with statements in refs. 12 and 13. Our results did not confirm, however, their claim that the energy difference is smaller than the twice of the spin gap so that the  $S = 2$  state is a stable bound state composed of the lowest excited state. What we read from Figs. 3-5 is that  $E - E_0$  for  $S = 2$  is located slightly above the twice of that for  $S = 1$ .

Before proceeding to the next section we would like to make a comparison between our results and the experimental data for  $\text{SrCu}_2(\text{BO}_3)_2$ . The energy of the lowest excited state with  $S = 1$ , namely the spin gap, can be determined in a very reliable manner both in experiments and in numerical works. The spin gap for this matter is established to be 3.0 meV (24.2  $\text{cm}^{-1}$ , 34.7 K) through various experiments.<sup>4, 16, 17)</sup> Another reliable quantity shared by experimental and theoretical investigations would be the energy of the lowest excited state with  $S = 0$ , which is reported to be 30  $\text{cm}^{-1}$  (3.7 meV) in the Raman scattering experiment.<sup>15)</sup> According to Knetter *et al.*,<sup>14)</sup> the observed energy is that of the SD=- state (the *odd*  $U$  parity state in our terminology) because the SD=+ state, which has the lower energy, is forbidden in this experiment. Among our trial states with  $S = 0$  and  $\mathbf{p}=(0,0)$  shown in the Appendix D, the *odd*  $U(=I_-V_x)$  ones are  $|\Psi_{nn,0,(0,0),a'}\rangle$ ,  $|\Psi_{nnn,0,(0,0),b'}\rangle$  and  $|\Psi_{nnn,0,(0,0),c'}\rangle$  while  $|\Psi_{nn,0,(0,0),b'}\rangle$ ,  $|\Psi_{nnn,0,(0,0),a'}\rangle$  and  $|\Psi_{nnn,0,(0,0),d'}\rangle$  have the *even*  $U$  parity. What we observe are that the lowest (the second lowest) energy is  $E_{nn,0,(0,0),a'}$  ( $E_{nn,0,(0,0),b'}$ ) if the coupling ratio is less than or equal to 0.8 (0.7). Thus, although we plot  $E_{nn,0,(0,0),a'}$  in Fig. 2, we should examine  $E_{nn,0,(0,0),b'}$  here. Requesting that the ratio  $(E_{nn,0,(0,0),b'} - E_0)/(E_{nn,1,(0,0),c'} - E_0)$  should be equal to the experimental value  $3.7/3.0 = 1.23$ , where  $E_{nn,1,(0,0),c'}$  is the lowest energy with  $S = 1$ , we fix  $J'/J$  for  $\text{SrCu}_2(\text{BO}_3)_2$  is 0.65 and  $J = 87\text{K}$ . These values are very close to those estimated by in ref.29, which are 0.635 and 85K, respectively.

Table 1 lists up our results for  $S \leq 1$  at  $J'/J = 0.65$  which are the lowest energy with different symmetries. From Table I we can further estimate, using the value  $J = 87\text{K}$ , that the energy difference of the *odd*  $U$ , *even*  $I_+$  state (of the *odd*  $I_+I_-$  state) is about 6.8 meV (7.0 meV). These

might correspond to the  $S = 0$  state observed in the infrared experiment,<sup>16)</sup> whose energy is  $52 \text{ cm}^{-1}$  (6.4 meV), or the one in the Raman scattering,<sup>15)</sup> whose energy is  $56 \text{ cm}^{-1}$  (6.9 meV). We did not find, however, any  $S = 1$  state to explain the second excited state observed in the experiments<sup>4,17)</sup> with the energy 54.7K (4.71 meV). The reason would be that the OV method is a kind of variational approach where the higher excitations for each set of quantum numbers are difficult to calculate.

## 5. Summary and discussions

In this paper we made a report of the excited states of the SS model. We carried out numerical investigations using the OV method, a kind of variational method we have developed.<sup>19,20)</sup> Our results show that the dispersion of the lowest excited state with the total spin  $S = 1$  is quite small, which indicates the locality of the state, even when the coupling ratio  $J'/J$  is as large as 0.65. It provides a contrast to the perturbative results, where the small dispersion is observed only for small  $J'/J$ .<sup>10)</sup> Another noticeable feature in our observations is that, when we start from  $J'/J = 0.45$  and increase this ratio keeping the momentum  $\mathbf{p}=\mathbf{0}$ , the energy of the  $S = 0$  state decreases faster than the energy of the  $S = 1$  state to form a crossover near  $J'/J = 0.65$ . This crossover supports an existence of the helical order phase suggested in refs. 23 and 24. The upper bound of  $J'/J$  for the phase transition point between the orthogonal dimer phase and the helical order phase is 0.75 in this study. We also successfully estimate the values of  $J'/J$  and  $J$  from our results and the experimental data,  $J'/J = 0.65$  and  $J = 87\text{K}$  for  $\text{SrCu}_2(\text{BO}_3)_2$ , which are compatible with the preceding studies.<sup>14,29)</sup>

Since it is so far difficult to perform the next order ( $L_{\text{max}} = 4$ ) calculations, which would be the best way to figure out the errors in our results, let us here try to discuss the reliability of our data (labeled by OV hereafter) by comparing some of them with the perturbative results<sup>12-14)</sup> (PB12, PB13, PB14), with the values from the perturbative expansion on the spin gap up to the fifth order of  $J'/J$ <sup>13)</sup> (PBF) and with the results from the exact diagonalization of 24 or 16 site cluster (ED24, ED16). For the lowest  $S = 1$  state, we have 0.679 (OV), 0.685 (PBF), 0.6779 (ED24) and 0.6797 (ED16) at  $J'/J = 0.5$  while they are 0.402 (OV), 0.436 (PBF), 0.3676 (ED24) and 0.3836 (ED16) when  $J'/J = 0.65$ . In the similar analysis on the lowest excited state with  $S = 0$ , we obtain 0.93 (OV), 0.80 (PB12), 0.90 (PB13, PB14), 0.858 (ED24) and 0.817 (ED16) at  $J'/J = 0.5$  while they are 0.59 (OV), 0.55 (PB13), 0.50 (PB14), 0.432 (ED24) and 0.386 (ED16) when  $J'/J = 0.6$ . These results suggest that our data are quite reliable when  $J'/J \sim 0.5$  and for larger values of the coupling ratio they give us reasonable upper bounds of the energy difference, especially for the spin gap.

We did not observe any instability on the  $S = 1$  two triplet states for large  $J'/J$  in contrast to the report in refs.13 and 14. Because this is an important issue in connection with the existence

of the helical order phase, further study would be necessary before we draw a definite conclusion. Another physically intriguing phenomenon is the magnetization plateau of  $\text{SrCu}_2(\text{BO}_3)_2$ . It is so far an open question to explain the experimentally observed  $1/8$  plateau from a theoretical point of view.<sup>11,30)</sup> We hope our method is helpful to solve this problem.

## Appendix A: Ground state

It is known that the exact ground state  $|\Psi_0\rangle$  for  $J'/J \leq 0.68$  is the product of all singlet dimers,

$$|\Psi_0\rangle = \prod_{n_x, n_y=0}^{N_{eff}-1} |\text{singlet}(2n_x, 2n_y)\rangle \cdot |\text{singlet}(2n_x + 1, 2n_y + 1)\rangle,$$

with

$$\begin{aligned} |\text{singlet}(2n_x, 2n_y)\rangle &\equiv \\ \frac{1}{\sqrt{2}} \{ &|\uparrow(2n_x a + \frac{d}{2}, 2n_y a + \frac{d}{2})\downarrow(2n_x a - \frac{d}{2}, 2n_y a - \frac{d}{2})\rangle \\ &- |\downarrow(2n_x a + \frac{d}{2}, 2n_y a + \frac{d}{2})\uparrow(2n_x a - \frac{d}{2}, 2n_y a - \frac{d}{2})\rangle \}, \\ |\text{singlet}(2n_x + 1, 2n_y + 1)\rangle &\equiv \\ \frac{1}{\sqrt{2}} \{ &|\uparrow((2n_x + 1)a + \frac{d}{2}, (2n_y + 1)a - \frac{d}{2})\downarrow((2n_x + 1)a - \frac{d}{2}, (2n_y + 1)a + \frac{d}{2})\rangle \\ &- |\downarrow((2n_x + 1)a + \frac{d}{2}, (2n_y + 1)a - \frac{d}{2})\uparrow((2n_x + 1)a - \frac{d}{2}, (2n_y + 1)a + \frac{d}{2})\rangle \}. \end{aligned}$$

## Appendix B: Operators which create the triplet dimer states

We introduce the operators  $\hat{T}_j$  ( $j = 0, \pm 1$ ) which operate the dimer singlet state and create the triplet one,

$$\begin{aligned} \hat{T}_j(2n_x, 2n_y) |\text{singlet}(2n_x, 2n_y)\rangle &= |S_z = j(2n_x, 2n_y)\rangle, \\ \hat{T}_j(2n_x + 1, 2n_y + 1) |\text{singlet}(2n_x + 1, 2n_y + 1)\rangle &= |S_z = j(2n_x + 1, 2n_y + 1)\rangle, \end{aligned}$$

where

$$\begin{aligned} \hat{T}_1(2n_x, 2n_y) &\equiv \frac{1}{\sqrt{2}} \{ -\sigma^+(2n_x a + \frac{d}{2}, 2n_y a + \frac{d}{2}) + \sigma^+(2n_x a - \frac{d}{2}, 2n_y a - \frac{d}{2}) \}, \\ \hat{T}_1(2n_x + 1, 2n_y + 1) &\equiv \\ \frac{1}{\sqrt{2}} \{ &-\sigma^+((2n_x + 1)a + \frac{d}{2}, (2n_y + 1)a - \frac{d}{2}) + \sigma^+((2n_x + 1)a - \frac{d}{2}, (2n_y + 1)a + \frac{d}{2}) \}, \end{aligned}$$



$$\begin{aligned}
\hat{T}_{-1}(2n_x, 2n_y) &\equiv -\frac{1}{\sqrt{2}}\{-\sigma^-(2n_x a + \frac{d}{2}, 2n_y a + \frac{d}{2}) + \sigma^-(2n_x a - \frac{d}{2}, 2n_y a - \frac{d}{2})\}, \\
\hat{T}_{-1}(2n_x + 1, 2n_y + 1) &\equiv \\
&-\frac{1}{\sqrt{2}}\{-\sigma^-((2n_x + 1)a + \frac{d}{2}, (2n_y + 1)a - \frac{d}{2}) + \sigma^-((2n_x + 1)a - \frac{d}{2}, (2n_y + 1)a + \frac{d}{2})\}, \\
\hat{T}_0(2n_x, 2n_y) &\equiv -\frac{1}{2}\{-\sigma^z(2n_x a + \frac{d}{2}, 2n_y a + \frac{d}{2}) + \sigma^z(2n_x a - \frac{d}{2}, 2n_y a - \frac{d}{2})\}, \\
\hat{T}_0(2n_x + 1, 2n_y + 1) &\equiv \\
&-\frac{1}{2}\{-\sigma^z((2n_x + 1)a + \frac{d}{2}, (2n_y + 1)a - \frac{d}{2}) + \sigma^z((2n_x + 1)a - \frac{d}{2}, (2n_y + 1)a + \frac{d}{2})\}.
\end{aligned}$$

### Appendix C: States in the momentum space

We define the states in the momentum space as follows.

$$\begin{aligned}
|(p_x, p_y)A\rangle &\equiv \sum_{n_x, n_y} \exp(ip_x n_x + ip_y n_y) \hat{T}_1(2n_x, 2n_y) |\Psi_0\rangle, \\
|(p_x, p_y)B\rangle &\equiv \sum_{n_x, n_y} \exp(ip_x n_x + ip_y n_y) \hat{T}_1(2n_x + 1, 2n_y + 1) |\Psi_0\rangle, \\
|(p_x, p_y)AR2\rangle &\equiv \sum_{n_x, n_y} \exp(ip_x n_x + ip_y n_y) \hat{T}_1(2n_x, 2n_y) \hat{T}_1(2n_x + 1, 2n_y + 1) |\Psi_0\rangle, \\
|(p_x, p_y)AL2\rangle &\equiv \sum_{n_x, n_y} \exp(ip_x n_x + ip_y n_y) \hat{T}_1(2n_x, 2n_y) \hat{T}_1(2n_x - 1, 2n_y - 1) |\Psi_0\rangle, \\
|(p_x, p_y)BR2\rangle &\equiv \sum_{n_x, n_y} \exp(ip_x n_x + ip_y n_y) \hat{T}_1(2n_x + 1, 2n_y + 1) \hat{T}_1(2n_x + 2, 2n_y) |\Psi_0\rangle, \\
|(p_x, p_y)BL2\rangle &\equiv \sum_{n_x, n_y} \exp(ip_x n_x + ip_y n_y) \hat{T}_1(2n_x + 1, 2n_y + 1) \hat{T}_1(2n_x, 2n_y + 2) |\Psi_0\rangle, \\
|(p_x, p_y)AR1\rangle &\equiv \sum_{n_x, n_y} \exp(ip_x n_x + ip_y n_y) \cdot \\
&\{\hat{T}_1(2n_x, 2n_y) \hat{T}_0(2n_x + 1, 2n_y + 1) - \hat{T}_0(2n_x, 2n_y) \hat{T}_1(2n_x + 1, 2n_y + 1)\} |\Psi_0\rangle, \\
|(p_x, p_y)AL1\rangle &\equiv \sum_{n_x, n_y} \exp(ip_x n_x + ip_y n_y) \cdot \\
&\{\hat{T}_1(2n_x, 2n_y) \hat{T}_0(2n_x - 1, 2n_y - 1) - \hat{T}_0(2n_x, 2n_y) \hat{T}_1(2n_x - 1, 2n_y - 1)\} |\Psi_0\rangle, \\
|(p_x, p_y)BR1\rangle &\equiv \sum_{n_x, n_y} \exp(ip_x n_x + ip_y n_y) \cdot \\
&\{\hat{T}_1(2n_x + 1, 2n_y + 1) \hat{T}_0(2n_x + 2, 2n_y) - \hat{T}_0(2n_x + 1, 2n_y + 1) \hat{T}_1(2n_x + 2, 2n_y)\} |\Psi_0\rangle, \\
|(p_x, p_y)BL1\rangle &\equiv \sum_{n_x, n_y} \exp(ip_x n_x + ip_y n_y) \cdot \\
&\{\hat{T}_1(2n_x + 1, 2n_y + 1) \hat{T}_0(2n_x, 2n_y + 2) - \hat{T}_0(2n_x + 1, 2n_y + 1) \hat{T}_1(2n_x, 2n_y + 2)\} |\Psi_0\rangle,
\end{aligned}$$

$$\begin{aligned}
| (p_x, p_y)AR0 \rangle &\equiv \sum_{n_x, n_y} \exp(ip_x n_x + ip_y n_y) \cdot \\
&\{ \hat{T}_1(2n_x, 2n_y) \hat{T}_{-1}(2n_x + 1, 2n_y + 1) + \hat{T}_{-1}(2n_x, 2n_y) \hat{T}_1(2n_x + 1, 2n_y + 1) \\
&- \hat{T}_0(2n_x, 2n_y) \hat{T}_0(2n_x + 1, 2n_y + 1) \} | \Psi_0 \rangle, \\
| (p_x, p_y)AL0 \rangle &\equiv \sum_{n_x, n_y} \exp(ip_x n_x + ip_y n_y) \cdot \\
&\{ \hat{T}_1(2n_x, 2n_y) \hat{T}_{-1}(2n_x - 1, 2n_y - 1) + \hat{T}_{-1}(2n_x, 2n_y) \hat{T}_1(2n_x - 1, 2n_y - 1) \\
&- \hat{T}_0(2n_x, 2n_y) \hat{T}_0(2n_x - 1, 2n_y - 1) \} | \Psi_0 \rangle, \\
| (p_x, p_y)BR0 \rangle &\equiv \sum_{n_x, n_y} \exp(ip_x n_x + ip_y n_y) \cdot \\
&\{ \hat{T}_1(2n_x + 1, 2n_y + 1) \hat{T}_{-1}(2n_x + 2, 2n_y) + \hat{T}_{-1}(2n_x + 1, 2n_y + 1) \hat{T}_1(2n_x + 2, 2n_y) \\
&- \hat{T}_0(2n_x + 1, 2n_y + 1) \hat{T}_0(2n_x + 2, 2n_y) \} | \Psi_0 \rangle, \\
| (p_x, p_y)BL0 \rangle &\equiv \sum_{n_x, n_y} \exp(ip_x n_x + ip_y n_y) \cdot \\
&\{ \hat{T}_1(2n_x + 1, 2n_y + 1) \hat{T}_{-1}(2n_x, 2n_y + 2) + \hat{T}_{-1}(2n_x + 1, 2n_y + 1) \hat{T}_1(2n_x, 2n_y + 2) \\
&- \hat{T}_0(2n_x + 1, 2n_y + 1) \hat{T}_0(2n_x, 2n_y + 2) \} | \Psi_0 \rangle, \\
| (p_x, p_y)Ax2 \rangle &\equiv \sum_{n_x, n_y} \exp(ip_x n_x + ip_y n_y) \hat{T}_1(2n_x, 2n_y) \hat{T}_1(2n_x + 2, 2n_y) | \Psi_0 \rangle, \\
| (p_x, p_y)Ay2 \rangle &\equiv \sum_{n_x, n_y} \exp(ip_x n_x + ip_y n_y) \hat{T}_1(2n_x, 2n_y) \hat{T}_1(2n_x, 2n_y + 2) | \Psi_0 \rangle, \\
| (p_x, p_y)Bx2 \rangle &\equiv \sum_{n_x, n_y} \exp(ip_x n_x + ip_y n_y) \hat{T}_1(2n_x + 1, 2n_y + 1) \hat{T}_1(2n_x + 3, 2n_y + 1) | \Psi_0 \rangle, \\
| (p_x, p_y)By2 \rangle &\equiv \sum_{n_x, n_y} \exp(ip_x n_x + ip_y n_y) \hat{T}_1(2n_x + 1, 2n_y + 1) \hat{T}_1(2n_x + 1, 2n_y + 3) | \Psi_0 \rangle, \\
| (p_x, p_y)Ax1 \rangle &\equiv \sum_{n_x, n_y} \exp(ip_x n_x + ip_y n_y) \cdot \\
&\{ \hat{T}_1(2n_x, 2n_y) \hat{T}_0(2n_x + 2, 2n_y) - \hat{T}_0(2n_x, 2n_y) \hat{T}_1(2n_x + 2, 2n_y) \} | \Psi_0 \rangle, \\
| (p_x, p_y)Ay1 \rangle &\equiv \sum_{n_x, n_y} \exp(ip_x n_x + ip_y n_y) \cdot \\
&\{ \hat{T}_1(2n_x, 2n_y) \hat{T}_0(2n_x, 2n_y + 2) - \hat{T}_0(2n_x, 2n_y) \hat{T}_1(2n_x, 2n_y + 2) \} | \Psi_0 \rangle, \\
| (p_x, p_y)Bx1 \rangle &\equiv \sum_{n_x, n_y} \exp(ip_x n_x + ip_y n_y) \cdot \\
&\{ \hat{T}_1(2n_x + 1, 2n_y + 1) \hat{T}_0(2n_x + 3, 2n_y + 1) - \hat{T}_0(2n_x + 1, 2n_y + 1) \hat{T}_1(2n_x + 3, 2n_y + 1) \} | \Psi_0 \rangle, \\
| (p_x, p_y)By1 \rangle &\equiv \sum_{n_x, n_y} \exp(ip_x n_x + ip_y n_y) \cdot \\
&\{ \hat{T}_1(2n_x + 1, 2n_y + 1) \hat{T}_0(2n_x + 1, 2n_y + 3) - \hat{T}_0(2n_x + 1, 2n_y + 1) \hat{T}_1(2n_x + 1, 2n_y + 3) \} | \Psi_0 \rangle.
\end{aligned}$$

## Appendix D: Trial states in the $p_y = p_x$ case

Using the states defined in the previous section we construct trial states. We employ  $S_z = S = j$  ( $j = 0, 1, 2$ ) states described below as the trial states. It should be noted that some states are degenerate. In order to point out the degeneracy we use the notation  $E_m$  to represent the lowest energy obtained with the trial state  $|\Psi_m\rangle$ .

### D.1 one-triplet states ( $S = 1$ )

The trial states with one triplet are as follows.

$$\begin{aligned} |\Psi_{one,1,(p,p),a}\rangle &\equiv |(p,p)A\rangle \quad (I_+ \text{even}), \\ |\Psi_{one,1,(p,p),b}\rangle &\equiv |(p,p)B\rangle \quad (I_+ \text{odd}). \end{aligned}$$

Note that  $E_{one,1,(p,p),a} = E_{one,1,(p,p),b}$ .

The following should also be kept in mind in order to make a comparison between the numerical results and the experimental data.

$$\begin{aligned} I_- |\Psi_{one,1,(0,0),a}\rangle &= - |\Psi_{one,1,(0,0),a}\rangle, \quad V_x |\Psi_{one,1,(0,0),a}\rangle = - |\Psi_{one,1,(0,0),b}\rangle, \\ I_- |\Psi_{one,1,(0,0),b}\rangle &= + |\Psi_{one,1,(0,0),b}\rangle, \quad V_x |\Psi_{one,1,(0,0),b}\rangle = - |\Psi_{one,1,(0,0),a}\rangle. \end{aligned}$$

### D.2 two-nearest-neighboring-triplet states ( $S = j$ , $j = 0, 1, 2$ )

The trial states with two nearest neighboring triplets for  $p \neq 0$ ,  $p \neq \pi$  are

$$\begin{aligned} |\Psi_{nn,j,(p,p),a}\rangle &\equiv |(p,p)ARj\rangle \quad (I_+ \text{odd}), \\ |\Psi_{nn,j,(p,p),b}\rangle &\equiv |(p,p)ALj\rangle \quad (I_+ \text{odd}), \\ |\Psi_{nn,j,(p,p),c}\rangle &\equiv |(p,p)BRj\rangle + |(p,p)BLj\rangle \quad (I_+ \text{odd}), \\ |\Psi_{nn,j,(p,p),d}\rangle &\equiv |(p,p)BRj\rangle - |(p,p)BLj\rangle \quad (I_+ \text{even}). \end{aligned}$$

For the momentum (0,0) they are

$$\begin{aligned} |\Psi_{nn,j,(0,0),a'}\rangle &\equiv |(0,0)ARj\rangle + |(0,0)ALj\rangle + |(0,0)BRj\rangle + |(0,0)BLj\rangle \quad (I_+ \text{odd}), \\ |\Psi_{nn,j,(0,0),b'}\rangle &\equiv |(0,0)ARj\rangle + |(0,0)ALj\rangle - |(0,0)BRj\rangle - |(0,0)BLj\rangle \quad (I_+ \text{odd}), \\ |\Psi_{nn,j,(0,0),c'}\rangle &\equiv |(0,0)ARj\rangle - |(0,0)ALj\rangle \quad (I_+ \text{odd}), \\ |\Psi_{nn,j,(0,0),d'}\rangle &\equiv |(0,0)BRj\rangle - |(0,0)BLj\rangle \quad (I_+ \text{even}). \end{aligned}$$

Also for the momentum  $(\pi, \pi)$  they are

$$\begin{aligned} |\Psi_{nn,j,(\pi,\pi),a''}\rangle &\equiv |(\pi,\pi)ARj\rangle + |(\pi,\pi)ALj\rangle + i\{|(\pi,\pi)BRj\rangle + |(\pi,\pi)BLj\rangle\} \quad (I_+ \text{odd}), \\ |\Psi_{nn,j,(\pi,\pi),b''}\rangle &\equiv |(\pi,\pi)ARj\rangle + |(\pi,\pi)ALj\rangle - i\{|(\pi,\pi)BRj\rangle + |(\pi,\pi)BLj\rangle\} \quad (I_+ \text{odd}), \\ |\Psi_{nn,j,(\pi,\pi),c''}\rangle &\equiv |(\pi,\pi)ARj\rangle - |(\pi,\pi)ALj\rangle \quad (I_+ \text{odd}), \\ |\Psi_{nn,j,(\pi,\pi),d''}\rangle &\equiv |(\pi,\pi)BRj\rangle - |(\pi,\pi)BLj\rangle \quad (I_+ \text{even}). \end{aligned}$$

Note that  $E_{nn,j,(0,0),c'} = E_{nn,j,(0,0),d'}$  and  $E_{nn,j,(\pi,\pi),c''} = E_{nn,j,(\pi,\pi),d''}$ .

The following should also be kept in mind, too.

$$\begin{aligned} I_- | \Psi_{nn,j,(0,0),a'} \rangle &= - | \Psi_{nn,j,(0,0),a'} \rangle, & V_x | \Psi_{nn,j,(0,0),a'} \rangle &= + | \Psi_{nn,j,(0,0),a'} \rangle, \\ I_- | \Psi_{nn,j,(0,0),b'} \rangle &= - | \Psi_{nn,j,(0,0),b'} \rangle, & V_x | \Psi_{nn,j,(0,0),b'} \rangle &= - | \Psi_{nn,j,(0,0),b'} \rangle, \\ I_- | \Psi_{nn,j,(0,0),c'} \rangle &= + | \Psi_{nn,j,(0,0),c'} \rangle, & V_x | \Psi_{nn,j,(0,0),c'} \rangle &= - | \Psi_{nn,j,(0,0),d'} \rangle, \\ I_- | \Psi_{nn,j,(0,0),d'} \rangle &= - | \Psi_{nn,j,(0,0),d'} \rangle, & V_x | \Psi_{nn,j,(0,0),d'} \rangle &= - | \Psi_{nn,j,(0,0),c'} \rangle. \end{aligned}$$

### D.3 two-next-nearest-neighboring-triplet states ( $S = j$ , $j = 0, 1, 2$ )

When  $S = j'$  ( $j' = 0, 2$ ) and  $p = 0$ , the trial states with two-next-nearest-neighboring triplets are

$$\begin{aligned} | \Psi_{nnn,j',(0,0),a'} \rangle &\equiv | (0,0)Axj' \rangle + | (0,0)Ayj' \rangle + | (0,0)Bxj' \rangle + | (0,0)Byj' \rangle \quad (I_+ \text{even}), \\ | \Psi_{nnn,j',(0,0),b'} \rangle &\equiv | (0,0)Axj' \rangle + | (0,0)Ayj' \rangle - | (0,0)Bxj' \rangle - | (0,0)Byj' \rangle \quad (I_+ \text{even}), \\ | \Psi_{nnn,j',(0,0),c'} \rangle &\equiv | (0,0)Axj' \rangle - | (0,0)Ayj' \rangle + | (0,0)Bxj' \rangle - | (0,0)Byj' \rangle \quad (I_+ \text{odd}), \\ | \Psi_{nnn,j',(0,0),d'} \rangle &\equiv | (0,0)Axj' \rangle - | (0,0)Ayj' \rangle - | (0,0)Bxj' \rangle + | (0,0)Byj' \rangle \quad (I_+ \text{odd}). \end{aligned}$$

When  $S = 1$  and  $p = \pi$  they are

$$\begin{aligned} | \Psi_{nnn,1,(\pi,\pi),a''} \rangle &\equiv | (\pi,\pi)Ax1 \rangle + | (\pi,\pi)Ay1 \rangle + i\{ | (\pi,\pi)Bx1 \rangle + | (\pi,\pi)By1 \rangle \} \quad (I_+ \text{even}), \\ | \Psi_{nnn,1,(\pi,\pi),b''} \rangle &\equiv | (\pi,\pi)Ax1 \rangle - | (\pi,\pi)Ay1 \rangle - i\{ | (\pi,\pi)Bx1 \rangle + | (\pi,\pi)By1 \rangle \} \quad (I_+ \text{odd}), \\ | \Psi_{nnn,1,(\pi,\pi),c''} \rangle &\equiv | (\pi,\pi)Ax1 \rangle + | (\pi,\pi)Ay1 \rangle + i\{ | (\pi,\pi)Bx1 \rangle - | (\pi,\pi)By1 \rangle \} \quad (I_+ \text{even}), \\ | \Psi_{nnn,1,(\pi,\pi),d''} \rangle &\equiv | (\pi,\pi)Ax1 \rangle - | (\pi,\pi)Ay1 \rangle - i\{ | (\pi,\pi)Bx1 \rangle - | (\pi,\pi)By1 \rangle \} \quad (I_+ \text{odd}). \end{aligned}$$

Otherwise they are

$$\begin{aligned} | \Psi_{nnn,j,(p,p),a} \rangle &\equiv | (p,p)Axj \rangle + | (p,p)Ayj \rangle \quad (I_+ \text{even}), \\ | \Psi_{nnn,j,(p,p),b} \rangle &\equiv | (p,p)Axj \rangle - | (p,p)Ayj \rangle \quad (I_+ \text{odd}), \\ | \Psi_{nnn,j,(p,p),c} \rangle &\equiv | (p,p)Bxj \rangle + | (p,p)Byj \rangle \quad (I_+ \text{even}), \\ | \Psi_{nnn,j,(p,p),d} \rangle &\equiv | (p,p)Bxj \rangle - | (p,p)Byj \rangle \quad (I_+ \text{odd}). \end{aligned}$$

Note that  $E_{nnn,j',(\pi,\pi),a} = E_{nnn,j',(\pi,\pi),d}$ ,  $E_{nnn,j',(\pi,\pi),b} = E_{nnn,j',(\pi,\pi),c}$ , where  $j' = 0, 2$ , and  $E_{nnn,1,(0,0),a} = E_{nnn,1,(0,0),d}$ ,  $E_{nnn,1,(0,0),b} = E_{nnn,1,(0,0),c}$ ,  $E_{nnn,1,(\pi,\pi),a''} = E_{nnn,1,(\pi,\pi),c''}$  and  $E_{nnn,1,(\pi,\pi),b''} = E_{nnn,1,(\pi,\pi),d''}$ .

The following should be kept in mind, too ( $j' = 0, 2$ ).

$$I_- | \Psi_{nnn,j',(0,0),a'} \rangle = + | \Psi_{nnn,j',(0,0),a'} \rangle, \quad V_x | \Psi_{nnn,j',(0,0),a'} \rangle = + | \Psi_{nnn,j',(0,0),a'} \rangle.$$

$$\begin{aligned}
I_- | \Psi_{nnn,j',(0,0),b'} \rangle &= + | \Psi_{nnn,j',(0,0),b'} \rangle, & V_x | \Psi_{nnn,j',(0,0),b'} \rangle &= - | \Psi_{nnn,j',(0,0),b'} \rangle, \\
I_- | \Psi_{nnn,j',(0,0),c'} \rangle &= - | \Psi_{nnn,j',(0,0),c'} \rangle, & V_x | \Psi_{nnn,j',(0,0),c'} \rangle &= + | \Psi_{nnn,j',(0,0),c'} \rangle, \\
I_- | \Psi_{nnn,j',(0,0),d'} \rangle &= - | \Psi_{nnn,j',(0,0),d'} \rangle, & V_x | \Psi_{nnn,j',(0,0),d'} \rangle &= - | \Psi_{nnn,j',(0,0),d'} \rangle, \\
I_- | \Psi_{nnn,1,(0,0),a} \rangle &= - | \Psi_{nnn,1,(0,0),a} \rangle, & V_x | \Psi_{nnn,1,(0,0),a} \rangle &= - | \Psi_{nnn,1,(0,0),a} \rangle, \\
I_- | \Psi_{nnn,1,(0,0),b} \rangle &= + | \Psi_{nnn,1,(0,0),b} \rangle, & V_x | \Psi_{nnn,1,(0,0),b} \rangle &= - | \Psi_{nnn,1,(0,0),b} \rangle, \\
I_- | \Psi_{nnn,1,(0,0),c} \rangle &= - | \Psi_{nnn,1,(0,0),c} \rangle, & V_x | \Psi_{nnn,1,(0,0),c} \rangle &= - | \Psi_{nnn,1,(0,0),c} \rangle, \\
I_- | \Psi_{nnn,1,(0,0),d} \rangle &= + | \Psi_{nnn,1,(0,0),d} \rangle, & V_x | \Psi_{nnn,1,(0,0),d} \rangle &= - | \Psi_{nnn,1,(0,0),a} \rangle.
\end{aligned}$$

### Appendix E: Trial states in the $p_y = 0$ case

We limit ourselves to  $S = 1$  and  $p_x \neq 0$  here. The trial states are as follows.

#### E.1 one-triplet states

$$\begin{aligned}
| \Psi_{one,1,(p,0),a} \rangle &\equiv | (p,0)A \rangle + \exp\left(\frac{ip}{2}\right) | (p,0)B \rangle, \\
| \Psi_{one,1,(p,0),b} \rangle &\equiv | (p,0)A \rangle - \exp\left(\frac{ip}{2}\right) | (p,0)B \rangle.
\end{aligned}$$

Note that

$$V_y \{ | (p,0)A \rangle \pm \exp\left(\frac{ip}{2}\right) | (p,0)B \rangle \} = \pm \exp\left(-\frac{ip}{2}\right) \{ | (p,0)A \rangle \pm \exp\left(\frac{ip}{2}\right) | (p,0)B \rangle \}.$$

#### E.2 two-nearest-neighboring-triplet states

$$\begin{aligned}
| \Psi_{nn,1,(p,0),a} \rangle &\equiv | (p,0)AR \rangle + \exp\left(\frac{ip}{2}\right) | (p,0)BR \rangle, \\
| \Psi_{nn,1,(p,0),b} \rangle &\equiv | (p,0)AR \rangle - \exp\left(\frac{ip}{2}\right) | (p,0)BR \rangle, \\
| \Psi_{nn,1,(p,0),c} \rangle &\equiv | (p,0)AL \rangle + \exp\left(\frac{ip}{2}\right) | (p,0)BL \rangle, \\
| \Psi_{nn,1,(p,0),d} \rangle &\equiv | (p,0)AL \rangle - \exp\left(\frac{ip}{2}\right) | (p,0)BL \rangle.
\end{aligned}$$

Note that

$$V_y \{ | (p,0)AZ \rangle \pm \exp\left(\frac{ip}{2}\right) | (p,0)BZ \rangle \} = \pm \exp\left(-\frac{ip}{2}\right) \{ | (p,0)AZ \rangle \pm \exp\left(\frac{ip}{2}\right) | (p,0)BZ \rangle \},$$

with  $Z = L$  or  $Z = R$ .

Also note that  $E_{nn,1,(p,0),a} = E_{nn,1,(p,0),c}$  and  $E_{nn,1,(p,0),b} = E_{nn,1,(p,0),d}$ .

- 1) B.S.Shastry and B.Sutherland: *Physica* **108B** (1981) 1069.
- 2) H.Kageyama, K.Yoshimura, R.Stern, N.V.Mushnikov, K.Onizuka, M.Kato, K.Kosuge, C.P.Slichter, T.Goto and Y.Ueda: *Phys. Rev. Lett.* **82** (1999) 3168.
- 3) K.Onizuka, H.Kageyama, Y.Narumi, K.Kindo, Y.Ueda and T.Goto: *J. Phys. Soc. Jpn.* **69** (2000) 1016.
- 4) H.Kageyama, M.Nishi, N.Aso, K.Onizuka, T.Yoshihama, K.Nukui, K.Kodama, K.Kakurai and Y.Ueda: *Phys. Rev. Lett.* **84** (2000) 5876.
- 5) M.Hofmann, H.Kierspel, T.Lorenz, G.S.Uhrig, O.Zabara, A.Freimuth, H.Kageyama, and Y.Ueda: *Phys. Rev. Lett.* **87** (2001) 047202.
- 6) M.Hofmann, T.Lorenz, A.Freimuth, G.S.Uhrig, H.Kageyama, Y.Ueda, G.Dhalenne and A.Revcolevschi: *Physica B* **312-313C** (2002) 597.
- 7) S.Zherlitsyn, S.Schmidt, B.Wolf, H.Schwenk, B.Lüthi, H. Kageyama, K. Onizuka, Y. Ueda and K. Ueda: *Phys. Rev. B* **62** (2000) 6097.
- 8) S.Miyahara and K.Ueda: *Phys. Rev. Lett.* **82** (1999) 3701.
- 9) E.Müller-Hartman R.R.P.Singh, C.Knetter and G.S.Uhrig: *Phys. Rev. Lett.* **84** (2000) 1808.
- 10) Z.Weihong, C.J.Hamer and J.Oitmaa: *Phys. Rev.* **B60** (1999) 6608.
- 11) T.Momoi and K.Totsuka: *Phys. Rev.* **B61** (2000) 3231; *Phys. Rev.* **B62** (2000) 15067.
- 12) K.Totsuka, S.Miyahara and K.Ueda: *Phys. Rev. Lett.* **86** (2001) 520.
- 13) Y.Fukumoto: *J. Phys. Soc. Jpn.* **69** (2000) 2755.
- 14) C.Knetter, A.Bühler, E.Müller-Hartman and G.S.Uhrig: *Phys. Rev. Lett.* **85** (2000) 3958.
- 15) P.Lemmens, M. Grove, M. Fischer, G. Güntherodt, V. N. Kotov, H. Kageyama, K. Onizuka and Y. Ueda: *Phys. Rev. Lett.* **85** (2000) 2605.
- 16) T. Rößm, U. Nagel, E. Lippmaa, H. Kageyama, K. Onizuka and Y. Ueda: *Phys. Rev.* **B61** (2000) 14342.
- 17) H.Nojiri, H.Kageyama, K.Onizuka, Y.Ueda and M. Motokawa: *J. Phys. Soc. Jpn.* **68** (1999) 2906.
- 18) K.Kodama, J.Yamazaki, M.Takigawa, H.Kageyama, K.Onizuka and Y.Ueda: *cond-mat/0203426*.
- 19) T. Munehisa and Y. Munehisa: *J. Phys. Soc. Jpn.* **69** (2000) 2092.
- 20) T. Munehisa and Y. Munehisa: *Comput. Phys. Comm.* **142** (2001) 176.
- 21) T. Munehisa and Y. Munehisa: *Phys. Rev.* **B49** (1994) 3347; *Prog. Theor. Phys.* **92** (1994) 309; *Prog. Theor. Phys.* **93** (1995) 251; *Prog. Theor. Phys.* **96** (1996) 59.
- 22) T. Munehisa and Y. Munehisa: *J. Phys. Soc. Jpn.* **66** (1997) 3876.
- 23) A.Koga and N.Kawakami: *Phys. Rev. Lett.* **84** (2000) 4461.
- 24) M.Albrecht and F.Mila: *Europhys. Lett.* **34** (1996) 145.
- 25) Results calculated on a  $4 \times 4$  lattice did show size effects.
- 26) With the order  $L_{max}$  higher than 3 one might observe the finite size effects on these lattices.
- 27) Note that  $r_2$  should be less than or equal to  $r_1$  if there were no helical order phase.
- 28) We also examined the eigenvector of the effective Hamiltonian to make sure that those components which include the *nnn*-triplets stay dominant.
- 29) S.Miyahara and K.Ueda: Supplement B *J. Phys. Soc. Jpn* **69** (2000) 72.
- 30) Y.Fukumoto: *J. Phys. Soc. Jpn.* **70** (2001) 1397.

trial state $ \Psi_m\rangle$	S	$I_+$	$I_-$	$U$	$(E_m - E_0)/J$
$ \Psi_{nn,0,(0,0),a'}\rangle$	0	—	—	—	0.49
$ \Psi_{nn,0,(0,0),b'}\rangle$	0	—	—	+	0.40
$ \Psi_{nn,0,(0,0),c'}\rangle$	0	—	+	*	0.93
$ \Psi_{nn,0,(0,0),d'}\rangle$	0	+	—	*	0.93
$ \Psi_{nnn,0,(0,0),a'}\rangle$	0	+	+	+	0.80
$ \Psi_{nnn,0,(0,0),b'}\rangle$	0	+	+	—	0.91
$ \Psi_{nn,1,(0,0),a'}\rangle$	1	—	—	—	0.89
$ \Psi_{nn,1,(0,0),b'}\rangle$	1	—	—	+	1.04
$ \Psi_{nn,1,(0,0),c'}\rangle$	1	—	+	*	0.40
$ \Psi_{nn,1,(0,0),d'}\rangle$	1	+	—	*	0.40

Table I. The lowest energy for the trial states with different quantum numbers at the coupling ratio  $J'/J = 0.65$ . Asterisks (\*) in the table denote that the state is not an eigenstate of the operator  $U$ .

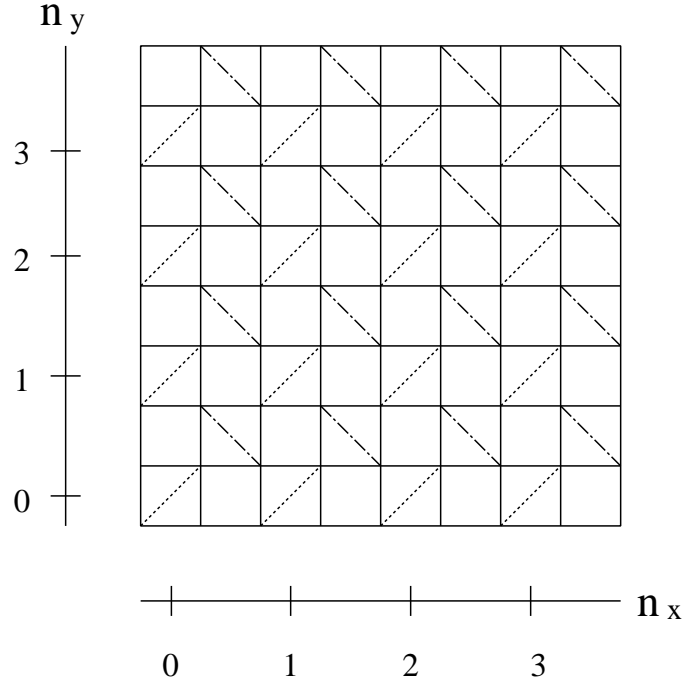


Fig. 1. A schematic view of the Shastry-Sutherland model. Each site is occupied by a spin. The intra-dimer coupling is denoted by dotted lines (A-sublattice) or dot-dashed lines (B-sublattice) and the inter-dimer coupling by solid lines.

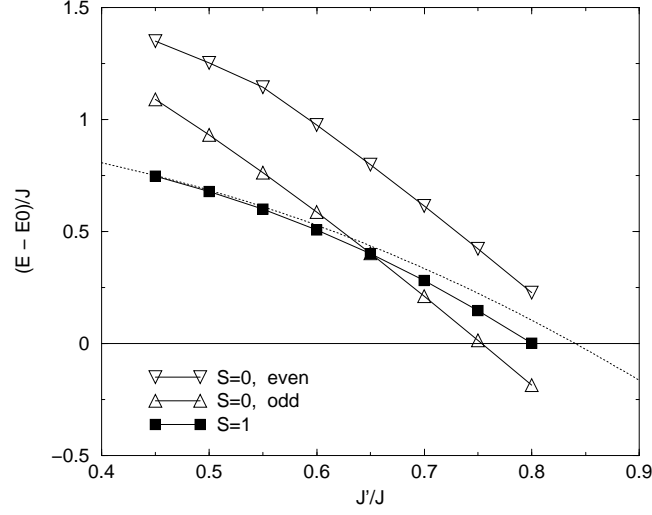


Fig. 2. Difference between  $E_0 = -\frac{3}{8}NJ$  (the energy of the singlet-dimer state) and the lowest energy obtained from the trial states with the momentum  $(0,0)$ . The dotted line is the spin gap estimated by the perturbation theory up to the fifth order,<sup>13)</sup>  $\Delta/J = 1 - (J'/J)^2 - \frac{1}{2}(J'/J)^3 - \frac{1}{8}(J'/J)^4 + \frac{2}{32}(J'/J)^5$ .

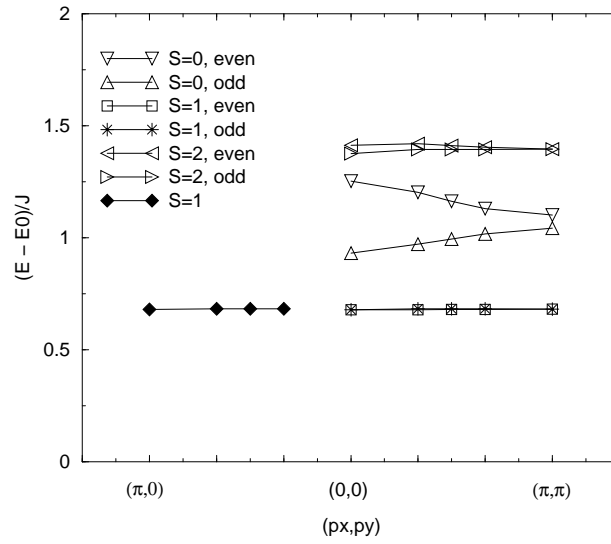
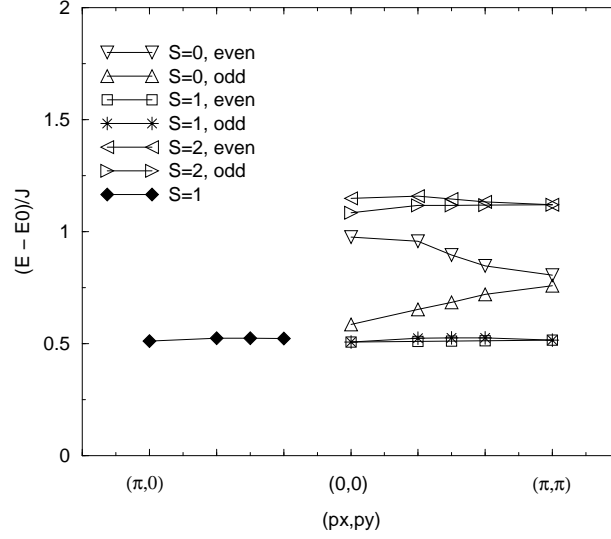
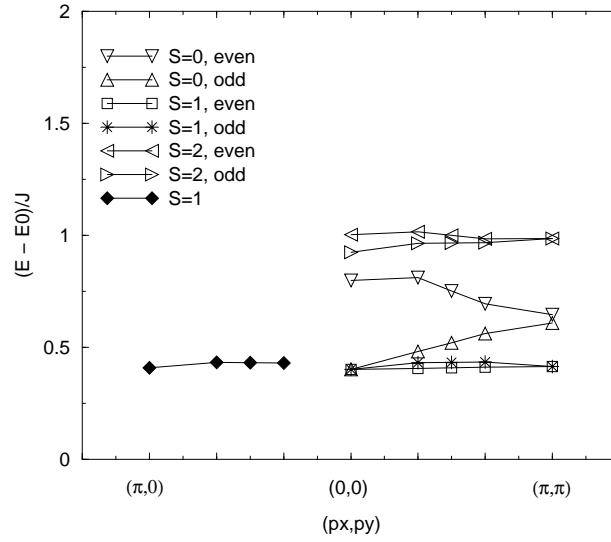


Fig. 3. Dispersion of the energy difference when the coupling ratio  $J'/J = 0.5$ .



Fig. 4. Dispersion of the energy difference when  $J'/J = 0.6$ .Fig. 5. Dispersion of the energy difference when  $J'/J = 0.65$ .